Proceedings of the 21st ICSMGE, Vienna, Austria, 14 – 19 June 2026. Pistrol, Adam & Schweiger (eds.)
Published by: ÖGG, Austrian Society for Geomechanics, Salzburg, Austria, ISBN 978-3-9503898-4-5
https://doi.org/10.53243/ICSMGE2026-1375

Site effect of deep alluvial soils: a case study in Batumi, Georgia

Hande Yumuk Ceylan, Hidayet Kemal Uyar, Emel Sıkıcı, Hilmi Turan Durgunoglu
Geotechnical Department, Zemin Etud ve Tasarım A.S., Türkiye, hande.yumuk@zeminas.com.tr

Onder Akcakal
Geotechnical Department, Zetas Zemin Teknolojisi A.S., Türkiye

ABSTRACT: The Batumi region of Georgia stands out as an area of active tectonics characterized by low to moderate-magnitude earthquakes. The deep alluvial soils in Batumi's coastal areas significantly alter the amplitude and frequency content of earthquake waves reaching the surface. In this study, the design acceleration spectrum for a high-rise building planned to be constructed 150 meters from the coastline in Batumi was derived using both Probabilistic Seismic Hazard Analysis (PSHA) and Site Response Analysis (SRA). The results were compared, leading to the selection of the final spectrum. Field investigations included Microtremor (MT) surveys, Multichannel Analysis of Surface Waves (MASW), Vertical Electrical Sounding (VES), and PS Logging, complemented by deep borehole drilling. However, the bedrock was not encountered during these investigations, leaving its depth and characteristics uncertain. To address this, multiple soil profiles were developed to represent the local ground conditions, and each profile was incorporated into the calculations for the design spectrum. In the PSHA studies, surface spectra for each idealized soil profile and base spectra for various bedrock shear wave velocities (Vs) were obtained. Bedrock depth was estimated by interpreting the dominant soil period (Tf) derived from MT studies, using iterative linear analyses where bedrock depth and properties were treated as variables. The bedrock's shear wave velocity was determined as the Vs value that produced the most critical surface spectrum. Following the determination of bedrock characteristics, detailed nonlinear SRA analyses were performed on the idealized soil profiles, and the resulting spectra were compared with those from PSHA. Despite the comprehensive field investigations, the study revealed significant uncertainties regarding the bedrock properties. The findings emphasize the critical influence of deep alluvial deposits on surface spectra and discuss the differences between results obtained from PSHA and SRA methods.

KEYWORDS: Batumi, Deep Alluvial Soils, Probabilistic Seismic Hazard Analysis (PSHA), Site Response Analysis (SRA), Design Acceleration Spectrum.

INTRODUCTION

The Batumi region of Georgia lies within an active tectonic zone characterized by low- to moderate-magnitude earthquakes, located in the Caucasus Orogen near the active tectonic belts adjacent to the Turkish border. Batumi is influenced by the eastern extensions of the Eastern Black Sea Fault System and the North Anatolian Fault. Both shallow crustal earthquakes and deep-focus Caucasus earthquakes are observed in the vicinity. The Batumi Cape belongs to the group of accumulative morphological forms and is primarily composed of continental deposits from the Rv. Chorokhi River. The river's course through the central part of Batumi city, combined with the presence of thick alluvial layers, emphasizes the importance of detailed geotechnical and seismotectonic investigations in the area.

The 14 January 1999 Turkey earthquake (Mw ≈ 6.0) disrupted seabed stability along the Batumi coastline, with sediment slides reported near the Chorokhi submarine canyon. In Batumi, design spectra for engineering purposes are generally derived by combining international PSHA models (GEM, USGS, ESHM) with local site measurements (microtremor, MASW, borehole data). Georgia does not yet have a detailed national seismic hazard map comparable to the one developed by AFAD in Turkey. Deep alluvial deposits in the coastal zone significantly alter the amplitude and frequency content of seismic waves reaching the surface.

In this study, the design acceleration spectra for a high-rise building (site located 150 m from the Batumi coastline was developed using both Probabilistic Seismic Hazard Analysis (PSHA) and Site Response Analysis (SRA), and the results were compared to determine the final spectra.

2 GEOLOGY AND SITE INVESTIGATIONS

2.1 Geology Of Batumi

Batumi is located in the southwestern part of Georgia, on the Black Sea coast, within the western segment of the Achara-Trialeti fold belt of the Lesser Caucasus. The region forms part of the active tectonic zones of the Caucasus Orogen and is influenced by the Eastern Black Sea Fault System and the eastern extensions of the North Anatolian Fault. Lithological, the area is characterized by Paleocene–Eocene volcanic and volcaniclastic rocks, overlain by Quaternary alluvial deposits (Figure 1). Batumi has developed on the delta of the River Chorokhi, where deltaic sediments consist of thick, heterogeneous alluvial layers. These deposits generally start with coarse materials such as sand, gravel, and cobbles near the surface, grading downward into fine-grained silt and clay layers.

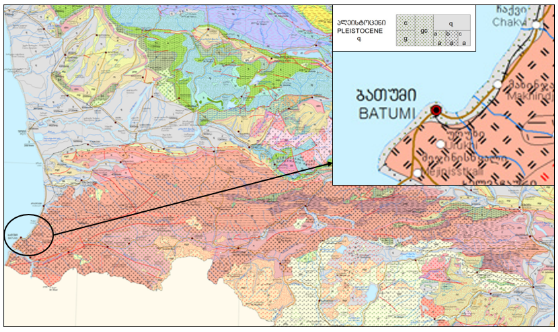

Figure 1. 1/500000 scaled geological map of Georgia, 2004.

Locally, remnants of former river channels and lacustrine–swamp deposits form weaker soil layers. The surficial geology reflects an alternation of marine and continental depositional environments, with the basaltic bedrock expected at depths of approximately 100–190 m.

2.2 Site Investigation

The field investigations, conducted in May 2024, comprised both geotechnical and geophysical studies (Table 1). A total of seven (7) boreholes were drilled using the rotary system, reaching a combined depth of (each 75-110m depth) 410.0 m. Standard Penetration Tests (SPT) were performed at 1.5 m intervals in accordance with ASTM D1586, utilizing an automatic hammer, and representative disturbed and undisturbed samples were obtained. Menard pressuremeter tests were carried out at twenty-three (23) selected depths, and constant-head permeability tests indicated an average hydraulic conductivity on the order of 10^{-2} m/s. Groundwater levels were monitored twice daily, with measured depths ranging from 2.95 m to 3.40 m below the existing ground surface.

The geophysical survey program included seismic refraction and active-source Multi-Channel Analysis of Surface Waves (MASW) along three (3) profiles, yieldng V_{S30} values between 303 m/s and 327 m/s, dominant periods (T_0) of 0.57–0.61 s, and site amplification factors of 2.11–2.21. In addition, three (3) microtremor measurements were conducted using the Nakamura method to determine the fundamental period and amplification characteristics.

Table 1. Summary soil investigation.

Investigation Method	Quantity	Depth Range / Interval	Notes / Key Results
Rotary Drilling	7 BH	Total depth: 410.0 m	No bedrock encountered
Standard Penetration Test (SPT)	All BH	1.5 m intervals	ASTM D1586, automatic hammer
Menard Pressuremeter Test	23 nos	Selected depths in BH	EM and PL values obtained
Constant-Head Permeability Test	10nos	2 Boreholes each 3meters depth till 20m	Hydraulic conductivity ≈ 10^{-2} m/s
MASW & Seismic Refraction	3 lines	Active-source method for near surface layers	V_{S30}: 303–327 m/s, T_0: 0.57–0.61 s, Ak: 2.11–2.21
Microtremor (H/V) Analysis	3 points	Fundamental period and amplification values obtained	Frequency 0.6296Hz-0.6488Hz-0.916Hz T_0:1.09-1.58
Vertical Electrical Sounding (VES)	3 sets	Schlumberger array	Profile length: 100–200 m; 22.08–365.61 Ω·m; mostly Less/Partially Corrosive; Highly Corrosive zone near surface
Suspension PS Logging	2 BH	1.0 m intervals	BH-1: depth 105.0 m, V_{S30} = 221 m/s; BH-2: depth 75.06 m, V_{S30} = 249 m/s; no bedrock.

Vertical Electrical Sounding (VES) surveys were undertaken at three (3) locations using the Schlumberger array to determine layer thicknesses and resistivity contrasts. Profiles of 100–200 m in length were measured, with resistivity values ranging from 22.08 Ω·m to 365.61 Ω·m. Corrosion classifications were predominantly Less Corrosive and Partially Corrosive, with a Highly Corrosive zone detected near the surface. These findings indicate spatial variability in the corrosion potential of the site soils, with some near-surface, low-resistivity layers presenting a high corrosion risk.

Downhole Suspension PS Logging was performed in two (2) boreholes at 1.0 m intervals. In the first borehole, measurements were carried out to a depth of 105.0 m, yielding a calculated V_{S30} of 221 m/s. In the second borehole, measurements extended to a depth of 75.06 m, with a V_{S30} of 249 m/s. P- and S-wave velocity profiles were obtained in both boreholes, and dynamic elastic parameters—including shear modulus, Young's modulus, and bulk modulus—were calculated. In both cases, no bedrock was encountered, and the results indicate that the subsoil profile consists predominantly of thick alluvial deposits of medium to low stiffness.

2.3 Local Geology

Across the site, from the surface to an average depth of approximately 40 m, dark grey to black, fine- to coarse-grained, angular to subangular sandy gravel and gravelly sand units are prevalent, ranging from loose to medium dense and very dense in nature. In borehole SK-1, this unit extends to a depth of 33 m, whereas in SK-4 and SK-5, its thickness increases towards the shoreline, reaching 48–54 m. Underlying this layer are dark grey to black, low- to high-plasticity, very stiff to hard silty clay units. In some areas, these clays contain sand lenses, and the silt content increases locally.

In borehole SK-4, a gravel/sand layer was observed between depths of 60 m and 67 m. The sands at this level are dark grey, fine- to coarse-grained, medium dense, and clayey-silty, while the gravels are angular to subangular and derived from various sources. In some intervals, shell fragments are present. Beneath this, further silty clay layers occur, characterized by low to medium plasticity, very stiff consistency, and occasional sand lenses. At greater depths, the clay layers show an increased silt content, interbedded with sand layers.

The investigations were carried out to a maximum depth of 108.5 m (elevation –104.5 m), and no bedrock formations were encountered at this depth.

3 PROBABILISTIC SEISMIC HAZARD ANALYSES (PSHA)

The primary objective of the PSHA studies was to develop site-specific acceleration spectra for the Batumi coastal project area, incorporating epistemic uncertainties in subsurface conditions identified through geophysical investigations.

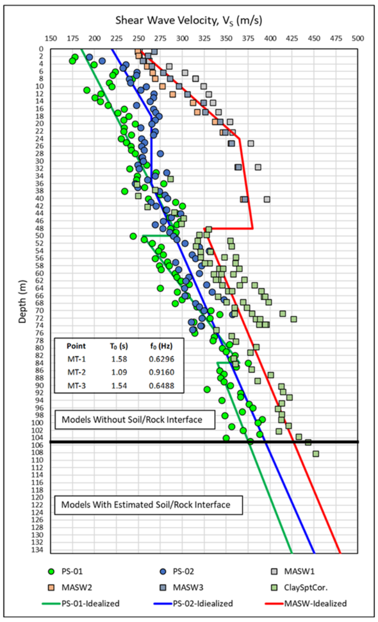

Figure 2. Summary of geophysical studies and related Vs profiles.

The specific aims were to:

- Determine the critical shear wave velocity (Vs) profile (Figure 2)
- Estimate the depth and characteristics of the bedrock
- Conduct probabilistic seismic hazard calculations and deaggregation analysis
- Identify scenario earthquakes for deterministic evaluations

- Obtain MCER, Design, and 10% PoE in 50 years spectra in accordance with ASCE 7-16
- Select and scale ground motion records compatible with the adopted bedrock spectra

The site investigation program included 3 MASW profiles, 2 Downhole Suspension PS-Logging measurements, and 3 Microtremor (MT) tests. Based on the PS-01, PS-02, and MASW data, three idealized Vs profiles were created to represent epistemic uncertainty.

3.1 Input Data and Geotechnical Constraints

Initial estimates from previous studies suggested the soil–rock interface to be located at ~120 m depth. Sequential linear elastic frequency-domain site response analyses (DeepSoil) were performed to refine bedrock depth estimates by comparing Fourier Amplitude Ratios (FAR) from one-dimensional models with microtremor observations (Figure 3).

For each idealized profile (PS-01, PS-02, MASW), the highest measured Vs value was initially assigned as the bedrock velocity. Profiles were then extended downward with an assumed velocity gradient until reaching Vs = 800 m/s, after which the analyses were repeated. The comparison with MT data identified two calibrated site profiles for subsequent hazard and site response analyses:

- PS-01: Vs_{30} = 211 m/s – lower natural frequency, higher amplification
- MASW: Vs_{30} = 312 m/s – higher natural frequency, lower amplification

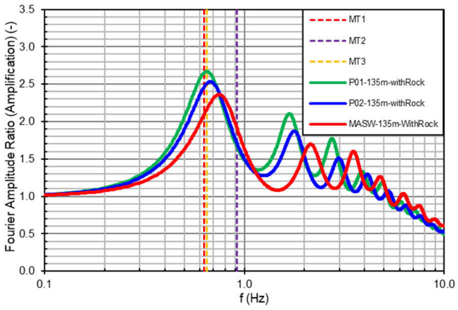

Figure 3. Site response analyses with estimated soil/rock interface.

3.2 Seismic Source Modelling and Logic Tree Approach

The PSHA was conducted using OpenQuake (Pagani et al., 2014) with supporting libraries HMTK, SMTK, and MBTK, alongside Zmap7 (Weimer, 2001). The modelling incorporated regional seismicity, mapped faults, and ground motion prediction equations (GMPEs), with logic tree weighting applied to control epistemic uncertainties.

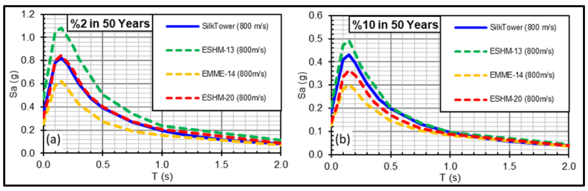

Figure 4. Rotd50 spectra calculated with different hazard models at the site.

Seismic source models were developed based on the European Seismic Hazard Map 2020 (ESHM20) (Danciu et al., 2021) and the Turkey Seismic Hazard Map Updating Project (TSTHG) (Akkar et al., 2014). Four distinct source models were considered (Figure 4 and Figure 5).

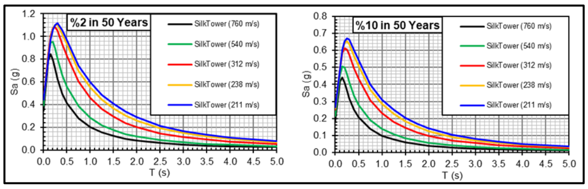

Figure 5. Rotd50 spectra calculated for soil and rock conditions in consider.

- ASM1 (TSTHG), ASM2 (ESHM20) – Area Source Models (ASM): Homogeneous seismicity within defined boundaries based on seismicity, fault characteristics, and geology.
- FSM (TSTHG) – Fault Source Model: Discrete linear fault segments with parameters from fault databases.
- F+SSM (ESHM20) – Fault + Spatially Smoothed Seismicity Model: Combination of mapped faults and weighted background seismicity not linked to specific faults.

In the logic tree, the weights were assigned as ASM – 50%, FSM – 25%, F+SSM – 25%. For area sources, maximum magnitude (M_{max}) values were treated as epistemic uncertainty; for fault sources, the bounds of slip rates were included similarly.

3.2 Base Rock Class Selection

Base spectra were generated using PSHA for two bedrock classes per ASCE 7-16: Class C: Vs = 540 m/s and Class BC: Vs = 760 m/s (Figure 6).

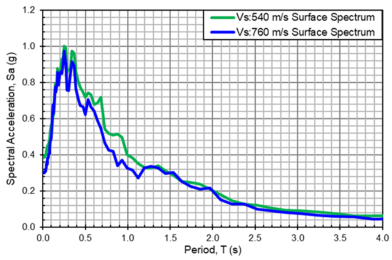

Figure 6. Surface spectra for different bedrock conditions.

Each base spectra were propagated through the site models. The Class C case (Vs = 540 m/s), as a result of linear elastic DeepSoil analysis, produced the more critical surface spectra and was therefore adopted for nonlinear Site Response Analysis (SRA).

3.3 Deaggregation Analysis and Deterministic Calculations

According to ASCE 7-22, the site-specific MCER spectral acceleration at any period (S_{aM}) is defined as the minimum of the values obtained from probabilistic and deterministic analyses. The deterministic spectrum is calculated as the 84th-percentile, 5% damped spectral acceleration in the direction of maximum horizontal response for scenario earthquakes determined through deaggregation of the probabilistic results. Only faults contributing at least 10% of the largest scenario earthquake at each period are considered (Figure 7).

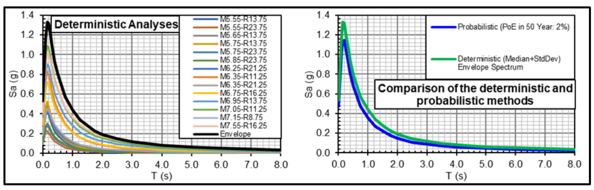

Figure 7. Deterministic scenario earthquakes and comparison to probabilistic method.

3.3 Results and Application

In this study, Maximum Considered Earthquake (MCER) is taken as the 5% damped acceleration response spectra that has a 2% probability of exceedance within a 50-year period. The design spectral response acceleration at any period is determined as 2/3 of the MCE values as recommended in ASCE 7-22.

The GMPE's used in this study predict the RotD50 of the two horizontal components of the acceleration spectra. For this reason, the RotD50 spectra scaled by factors suggested in ASCE 7-22 to determine MCER spectra (Figure 9).

ASCE 7-22 indicates that "Faults with estimated slip rate less than 1 mm per year shall not be used to determine whether a site is a near-fault site". Therefore, the site is not classified as a near fault site (Figure 8).

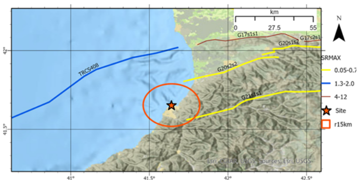

Figure 8. Closest faults to the site.

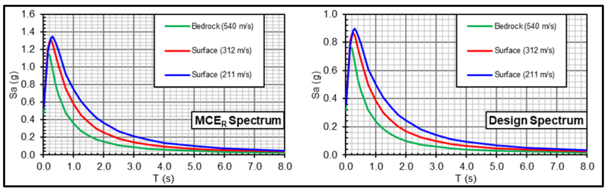

Figure 9. MCER and design spectra for surface and bedrock at the site.

The adopted bedrock unit for SRA is a weathered tuff with Vs = 540 m/s. PSHA-derived bedrock-level spectra for Vs = 540 m/s were used as input motions for both selected site profiles (V_{S30} = 211 m/s and V_{S30} = 312 m/s). The depth of the bedrock is estimated to be 135m, with a Vs shear wave velocity of 540 m/s.

Surface spectra from PSHA will be compared with the results of nonlinear SRA to determine the final recommended design spectra for the project. This approach ensures that both the lower-frequency/high-amplification and higher-frequency/low-amplification site conditions are explicitly considered in the seismic design (Figure 10).

Five individual earthquake records were selected and scaled to the MCER spectra to be used as input for the site response analysis (Figure 11).

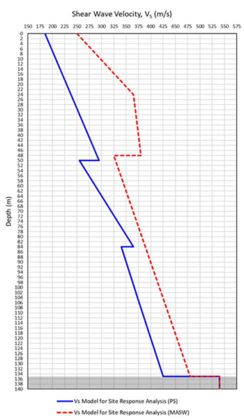

Figure 10. Idealized Vs profiles for nonlinear site response analysis.

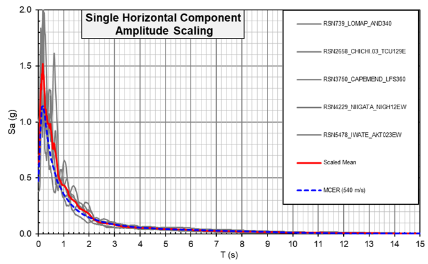

#	Event	Station	Mechanism	Mw	Rjb (km)	Vs30 (m/s)	Scale Factor
e1	"Loma Prieta"	"Anderson Dam"	Oblique	6.93	19.9	489	1.95
e2	"Chi-Chi Taiwan-03"	"TCU129"	Reverse	6.20	10.95	511	1.06
e3	"Cape Mendocino"	"Loleta Fire Station"	Reverse	7.01	23.46	516	1.46
e4	"Niigata_ Japan"	"NIGH12"	Reverse	6.63	9.93	564	2.01
e5	"Iwate_ Japan"	"AKT023"	Reverse	6.90	11.68	556	1.59

Figure 11. Acceleration spectra for scaled ground motions and target (MCER, 540 m/s) spectra.

4. SITE RESPONSE ANALYSES (SRA)

For the Site Response Analyses, the scope of work includes determining the critical shear wave velocity profile to bedrock, evaluating dynamic soil parameters, calibrating constitutive model parameters for undrained conditions, performing nonlinear site response analyses (SRA) using PSHA-derived bedrock properties and earthquake motions (MCE Level), and deriving the surface design spectra by integrating the results of PSHA and SRA.

4.1 Soil Behavior and Parameters

The idealized soil profile and recommended geotechnical parameters derived from site investigations are presented in Table 2 and Table 3. The idealized shear wave velocity (Vs) profile—previously used in site-specific probabilistic seismic hazard analyses (PSHA) was calibrated for the Hardening Soil (HS) Model in PLAXIS using Equation (1) which represents the PLAXIS- recommended formulation adapted from the work of Benz, T. (2006).

$$G_0 = G_0^{ref}\left(\frac{c\cos\varphi - \sigma_3'\sin\varphi}{c\cos\varphi + p_{ref}'\sin\varphi}\right)^m \quad (1)$$

The calibration results are shown in Figure 12, with the m coefficients enabling the required adjustments. For the analysis, MASW and PS logging results were assessed separately, and two distinct dynamic soil models were prepared (Table 2 and Table 3). In both cases, the rock depth was assumed to be 135 m below the surface, and results were evaluated collectively without modifying this depth assumption. The two model profiles are:

1. PS Logging-based profile: V_{S30} = 211 m/s
2. MASW-based profile: V_{S30} = 312 m/s

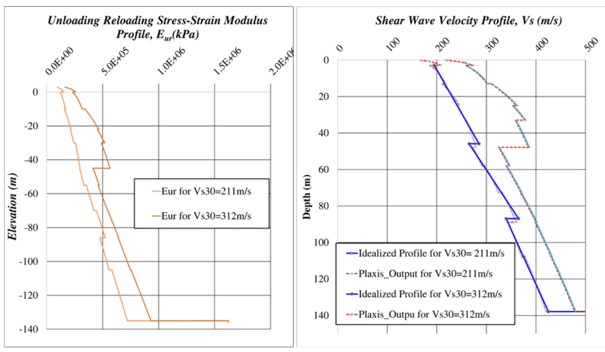

Figure 12. Calibration of E_{ur} values measured data idealization-model V_{s30}=312m/s and V_{s30}=211m/s.

Table 2. Geotechnical parameters of idealized soil profile for dynamic analyzes-model V_{s30}=211m/s.

Layer	Thickness	V_s	e	c'	ϕ'	$G_{o,ref}$	$\gamma_{0.7}$
Unit	m	m/s		kPa	°	MPa	-
Z1	2.88	195	0.84	1	33	55.1	7.5E-5
$Z1_{bulk}$	10.0	206	0.83	1	33	62.0	1.2E-4
Z2	12.0	230	0.79	1	31	78.9	1.6E-4
Z3	8.0	250	0.76	1	31	94.6	1.8E-4
Z4	15.0	270	0.68	10	30	115.9	2.6E-4
Z5	10.0	282	0.63	8	28	130.4	3.5E-4
Z6	15.0	312	0.61	9	30	161.3	3.2E-4
Z7	16.0	347	0.60	12	30	201.6	3.4E-4
Z8	19.0	358	0.59	11	28.5	215.2	4.0E-4
Z9	30.0	400	0.57	15	30	271.6	4.2E-4

Table 3. Geotechnical parameters of idealized soil profile for dynamic analyzes-model Vs30=312m/s.

Layer	Thickness	V_s	e	c'	ϕ'	$G_{o,ref}$	$\gamma_{0.7}$
Unit	m	m/s		kPa	°	MPa	-
Z1	2.88	255	0.84	1	33	94.2	8.0E-5
$Z1_{bulk}$	10.0	285	0.83	1	33	118.7	1.3E-4
Z2	12.0	338	0.79	1	31	169.9	1.6E-4
Z3	8.0	366	0.76	1	31	202.8	1.8E-4
Z4	15.0	372	0.68	10	30	220.1	2.6E-4
Z5	10.0	335	0.63	8	28	184.1	3.0E-4
Z6	15.0	355	0.61	9	30	208.9	3.2E-4
Z7	16.0	385	0.60	12	30	248.1	3.3E-4
Z8	19.0	415	0.59	11	28.5	289.2	4.0E-4
Z9	27.1	455	0.57	15	30	351.4	4.3E-4

3.3 Constitutive Models and Parameters

In dynamic analyses, the most critical parameter governing soil behavior is the initial shear modulus (G_0), calculated based on the shear wave velocity (V_s) and the soil's dynamic density. Using this modulus and the Poisson's ratio, the dynamic Young's modulus (E_0) is determined. Under static loading conditions, the relationship between dynamic moduli and loading–unloading moduli can be established according to Alpan (1970). The one-dimensional compression modulus (E_{oed}) and E_{50} can be approximately estimated as $E_{ur}/3$.

The Kelvin-Voigt model is used to describe the stress–strain relationship. During cyclic loading, the damping ratio (ξ) is employed to eliminate frequency dependence in energy dissipation. Equations show that the damping ratio significantly affects stress levels, making accurate damping ratio determination essential in dynamic analyses.

In this study, all soil units in the Plaxis software were analyzed using the Hardening Soil – Small Strain (HSS) constitutive model, which accounts for changes in stiffness and nonlinear behavior under dynamic loading. This model incorporates the hysteretic Masing Rule to simulate cyclic stress-strain behavior and calculates the damping ratio as a function of deformation. For the base unit, a Linear Elastic model was chosen.

Linear Elastic (LE) model is applied at the base unit to ensure accurate wave input and for verification purposes. When combined with Rayleigh damping, it allows viscoelastic analysis.

Hardening Soil with Small Strain (HSS) model accounts for stiffness variation and nonlinear behavior under dynamic loading. It incorporates the Masing rule to simulate hysteretic behavior and calculates damping ratio as a function of strain. G_0 is updated according to the prevailing stress state. Shear modulus reduction and damping curves are calibrated using Darendeli (2001) and Seed & Idriss (1970).

In the HSS model, the shear modulus reduction relationship is expressed based on the reference shear strain at which the initial modulus decreases to 70% of its value, as described by the Hardin & Drnevich (1972) curve (Figure 13).

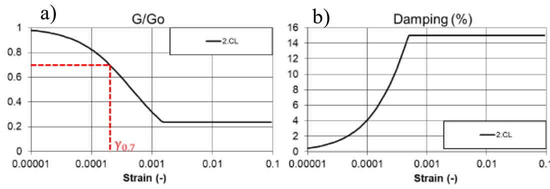

Figure 13. Comparison of results obtained from the Hardin-Drnevich relationship with test data by Santos & Correia (2001) in the HSS Model: (a) An example of shear modulus curves, b) An example of damping ratio curves.

For the calibration of the HSS model, in addition to calculating the parameters described earlier and shared in later sections of the report, the parameter γ0.7, which directly affects nonlinear behavior under earthquake loading, was selected to be consistent with the modulus reduction and damping ratio curves proposed by Darendeli (2001) and Seed & Idriss (1970) for sand soils.

As indicated by the damping ratio curves, the Hardin & Drnevich (1972) curves used in the HSS model show a damping ratio of 0 at small deformations, whereas Darendeli (2001) uses a minimum damping ratio Dmin. To address this limitation of the HSS model, a frequency-dependent Rayleigh Damping model was added to the hysteretic damping. The target damping ratio was set to 0.5% for soil units and 2% for the base unit. Using a higher Dmin ratio could lead to excessive damping in the model, while a lower value could result in unrealistic amplification of very high and very low-frequency components. While the target damping ratio is applied equally to each mode, the frequency values are determined based on the dominant soil frequency for f1 and the highest frequency content with significant amplitude in the earthquake records (Figure 14) applied to the model for f_2. Analyses were performed using the dynamic module of Plaxis 2D v2024 and the "Site Response" tool.

- Horizontal boundaries: "Compliant Base"
- Vertical boundaries: "Tied Degrees of Freedom"
- Five surface acceleration records in compliance with ASCE 7-22 were used.
- Maximum frequency fmax = 15 Hz, ensuring at least 8 elements per minimum wavelength in each layer.
- Time step: 0.0006 s.
- Model depth: 135 m, including a 134 m soil profile + 1 m elastic base.

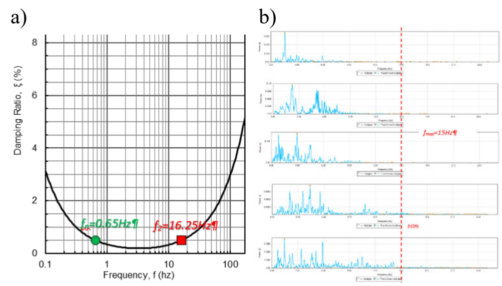

Figure 14. a) Rayleigh damping curve b) determination of maximum frequency

Since discrepancies were observed between different geophysical measurements, two separate dynamic models were developed to represent the site's average dynamic behavior. Surface design spectra were proposed based on the evaluation of results from both models.

The design spectral response acceleration at any period shall be determined from Equation (2) (ASCE-7, Equation (21.3-1)): where SaM is the MCER spectral response acceleration obtained from Site Response Analyzes or Risk-Targeted Maximum Considered Earthquake (MCER) Ground Motion Hazard Analyzes (Figure 15 and Figure 16).

$$S_a = \frac{2}{3} S_{aM} \tag{2}$$

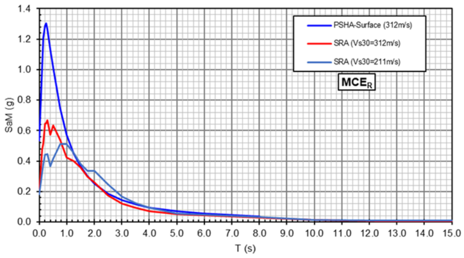

Figure 15. MCER response spectra's.

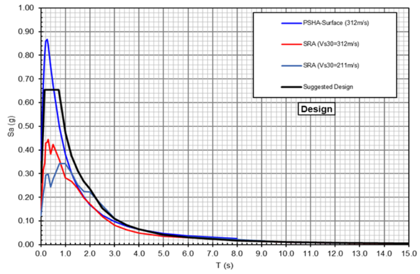

Figure 16. Design response spectrum and suggested design spectra.

4. CONCLUSIONS

Site-specific Probabilistic Seismic Hazard Analysis (PSHA) and nonlinear Site Response Analyses (SRA) were performed for a high-rise building located near the Batumi coastline, in accordance with the provisions of ASCE 7-16. Geophysical investigations, including MASW, Downhole Suspension PS-Logging, and microtremor measurements, were employed to develop and calibrate shear wave velocity profiles and to estimate the depth and dynamic properties of the underlying bedrock.

The Batumi region currently lacks a detailed seismic hazard map, and the project site is underlain by thick alluvial deposits of relatively low stiffness, which present significant challenges for high-rise construction. Boreholes drilled to depths of up to 110 m did not reach bedrock; therefore, its depth and key properties were inferred indirectly through geophysical methods. Under such geological conditions, site-specific seismic hazard and response analyses are essential to derive reliable design spectra and to ensure accurate seismic performance assessments.

For deep alluvial deposits hosting high-rise structures, the integration of microtremor array methods (e.g., SPAC, MT) with complementary geophysical investigations is strongly recommended to improve estimates of bedrock depth and dynamic soil behavior, thereby enabling the derivation of realistic surface spectra for design (Figure 16). This approach, as applied in the present study, is particularly valuable in regions where both detailed site investigation data and regional seismic hazard mapping are limited.

The recommended site-specific earthquake ground motion spectrum, derived from maximum RotD100 horizontal acceleration spectra at the surface under natural site conditions, provides a robust and technically defensible basis for seismic design of the planned structures. In accordance with applicable standards, structural engineers may alternatively adopt the MCER spectrum (Figure 15).

ACKNOWLEDGEMENTS

The authors would like to express their sincere gratitude to all the dedicated staff of Zemin Etüd ve Tasarım A.Ş. for their profound knowledge and commitment to research. Their expertise in geotechnical engineering, continuous technical support, and dedication to quality played a critical role in the successful completion of this project.

REFERENCES

Akkar, S., et al. 2014. Updating the Seismic Hazard Map of Turkey (TSTHG). Project Code UDAP-Ç-13-06, National Earthquake Research Program (UDAP). AFAD.

Alpan, I. 1970. The geotechnical properties of soils. Proceedings of the Istanbul Conference on Soil Mechanics and Foundation Engineering, Istanbul, pp. 1–14.

ASCE. 2016. Minimum Design Loads and Associated Criteria for Buildings and Other Structures (ASCE/SEI 7-16). Reston, VA: American Society of Civil Engineers.

ASCE. 2022. Minimum Design Loads and Associated Criteria for Buildings and Other Structures (ASCE/SEI 7-22). Reston, VA: American Society of Civil Engineers.

Benz, T. 2006. Small-strain stiffness of soils and its numerical consequences. PhD Thesis. Universität Stuttgart, IGS Mitteilungen No. 55.

Danciu, L., et al. 2021. The 2020 European Seismic Hazard Model (ESHM20). Bulletin of Earthquake Engineering, 19, pp. 4455–4477.

Darendeli, M.B. 2001. Development of normalized modulus reduction and material damping curves for generic soil types. PhD Dissertation. University of Texas at Austin.

Fung, Y.C. 1965. Foundations of Solid Mechanics. Englewood Cliffs: Prentice Hall.

Hardin, B.O. & Drnevich, V.P. 1972. Hyperbolic stress–strain response of granular soils. Journal of the Soil Mechanics and Foundations Division, ASCE, 98(SM7), pp. 667–692.

GEM Foundation. n.d. HMTK, SMTK, MBTK – Hazard Modeller's Toolkit, Strong Motion Toolkit, Model Builder's Toolkit. GEM Foundation.

Ibs-von Seht, M. & Wohlenberg, J. 1999. Microtremor measurements used to map thickness of soft sediments. Bulletin of the Seismological Society of America, 89(1), pp. 250–259.

Nakamura, Y. 1989. A method for dynamic characteristics estimation of subsurface using microtremor on the ground surface. Quarterly Report of RTRI, 30(1).

Pagani, M., et al. 2014. OpenQuake Engine: An Open Hazard (and Risk) Software for the Global Earthquake Model. Seismological Research Letters, 85(3), pp. 692–702.

PLAXIS. 2020. PLAXIS 2D Material Models Manual. Delft, Netherlands: Bentley Systems.

Santos, J.A. & Correia, A.G. 2001. Reference threshold shear strain of soil using bender elements. Experimental Techniques, 25(3), pp. 30–34.

Seed, H.B. & Idriss, I.M. 1970. Soil Moduli and Damping Factors for Dynamic Response Analyses. Report EERC 70-10. Earthquake Engineering Research Center, University of California, Berkeley.

SESAME Project. 2004. Guidelines for the implementation of the H/V spectral ratio technique on ambient vibrations. Deliverable D23.12.

Weimer, S. 2001. ZMAP: A MATLAB-Based Program Package for Analysis of Seismicity. Eos Transactions AGU, 82(47), Fall Meeting Supplement, Abstract S51A-02.